Resonant activation in a bistable system

M. Marchi,[1] F. Marchesoni,[2,3] L. Gammaitoni,[1,2] E. Menichella-Saetta,[1,4] and S. Santucci[1,4]
[1]*Dipartimento di Fisica, Universita' di Perugia, I-06100 Perugia, Italy*
[2]*Istituto Nazionale di Fisica Nucleare, VIRGO Project, Sezione di Perugia, I-06100 Perugia, Italy*
[3]*Dipartimento di Fisica, Universita' di Camerino, I-62032 Camerino, Italy*
[4]*Istituto Nazionale di Fisica della Materia, Unita di Perugia, I-06100 Perugia, Italy*
(Received 20 March 1996)

The analog simulation of an overdamped Brownian particle in a quartic double-well potential driven by an external (either Gaussian or dichotomic) multiplicative noise is performed with special focus on the phenomenon of resonant activation. Such an effect is shown to occur on increasing the correlation time of the multiplicative noise, while keeping the noise variance constant. The asymptotic behavior of the relevant escape times for large noise correlation time and large variance is also investigated. Simple qualitative arguments are produced to justify the results thus obtained. Furthermore, the traversal barrier, that is the effective barrier at the time the system switches state, is shown to have a minimum for a certain value of the noise correlation time, though not always in coincidence with the relevant resonant activation value. [S1063-651X(96)05610-3]

PACS number(s): 05.40.+j, 82.20.Mj

I. INTRODUCTION

The problem of thermally activated escape over randomly fluctuating barriers has been very popular among chemical physicists for at least fifty years now [1]. A surge of fresh interest in this topic was triggered recently by Doering and Gadoua [2], who studied how the interwell mean-first-passage time (MFPT) of a Brownian particle in a bistable potential depends on the correlation time τ of the barrier fluctuations. The observation that such a MFPT decreases for sufficiently small τ values and increases for asymptotically large τ values, led these authors to suggest that a resonant activation (RA) phenomenon occurs, quite independently of the details of the model considered. The basic ingredients of such a phenomenon are [3–12]: bistability, a weak additive noise (responsible for thermal activation), and a multiplicative noise with finite correlation time τ (modeling the barrier fluctuations). The earlier literature, which followed the Doering-Gadoua seminal paper, focused mostly on the solution of particularly simple models [3–6]; subsequently, a number of approximate schemes were envisaged to determine the MFPT as a function of τ for any choice of the bistable potential and barrier fluctuations [7–11]. The generality of the RA phenomenon was thus confirmed for a wide class of bistable systems.

In this article we conclude our analog simulation study of RA in the overdamped quartic double-well potential [12]

$$\dot{x} = -V'(x) + \xi(t) + x\,\eta(t), \tag{1.1}$$

with $V(x) = bx^4/4 - ax^2/2$ and $a,b>0$. Here, the additive Gaussian noise $\xi(t)$ represents the heat bath acting upon the Brownian particle with coordinate $x(t)$ and the force term corresponding to the fluctuating barrier is factorized into the product of a coupling function x, times a multiplicative noise $\eta(t)$. Both noise sources are assumed to be zero mean valued. The correlation time of $\xi(t)$ is kept negligibly short (namely, of the order of $10^{-2}\ a^{-1}$), whence $\langle \xi(t)\xi(0)\rangle = 2D\,\delta(t)$. Throughout the present report the strength of the additive noise D was kept much smaller than the unperturbed potential barrier height $E_0 = a^2/4b$. The correlation time of $\eta(t)$ is the control parameter of the system under investigation. The simplest correlation function for $\eta(t)$ one can simulate,

$$\langle \eta(t)\,\eta(t')\rangle = (Q/\tau)\exp(-|t-t'|/\tau) \tag{1.2}$$

suffices to provide a clear picture of the RA phenomenon. Two different $\eta(t)$ statistics were considered for the sake of comparison: (a) Gaussian [13]. The noise $\eta(t)$ is then a stationary Ornstein-Uhlenbeck noise with variance $\sigma^2 = Q/\tau$; (b) dichotomic [14]. The noise $\eta(t)$ flips between the constant values $\pm\sigma$ with waiting times distributed according to a Poisson law with time constant 2τ.

The direct measurement of the MFPT in our analog simulator turned out to be a rather cumbersome matter [12,13]. In fact, for $\sigma \ll a$ two (sometimes, more) exponential decay time constants are clearly distinguishable in $\langle x(t)x(0)\rangle$, whereas for extremely large τ values the very existence of an exponential tail becomes questionable [7]. For this reason we resorted to define the escape time $T(\tau,\sigma)$ as

$$T(\tau,\sigma) = \int_0^\infty dt \langle x(t)x(0)\rangle / \langle x^2\rangle, \tag{1.3}$$

where $\langle x(t)x(0)\rangle$ is the stationary autocorrelation function of the process $x(t)$. The connection between $T(\tau,\sigma)$ and the relevant MFPT is not straightforward for $\tau>0$ [19]: for weak color $a\tau \ll 1$ and low noise intensities $Q \ll a$, the MFPT for x to diffuse from one potential minimum up to the barrier top is well reproduced by Eq. (1.3). In fact, large τ and/or Q values may modify the bimodal dynamics of the unperturbed $[\eta(t)=0]$ thermal process $x(t)$ (see Fig. 8 of Sec. III); the notion of MFPT is, then, ill defined, whereas $T(\tau,\sigma)$ keeps defining consistently the process relaxation time, no matter what the $\eta(t)$ parameters. In the present report we try to adapt the MFPT formalism in order to approximate $T(\tau,\sigma)$ under different color and noise intensity regimes.

The outline of the present paper is as follows. In Sec. II we summarize the theoretical background required to analyze the results of our simulation work. In Sec. III the onset of RA is illustrated by plotting $T(\tau,\sigma)$ versus τ with either σ or Q constant and versus σ with τ constant. A number of intriguing features are thus revealed both for the Gaussian and the dichotomic statistics of the multiplicative noise, which elude any theoretical scheme proposed so far [2–11]. In Sec. IV most of the asymptotic behaviors are interpreted by means of simple intuitive arguments. In Sec. V the RA phenomenon is investigated by introducing the notion of traversal barrier E, defined as the effective barrier the Brownian particle overcomes at the time it crosses the separatrix $x=0$; here, a minimum of E is not always a direct signature of RA. The generality of the RA phenomenon is discussed further in Sec. VI.

II. THEORETICAL BACKGROUND

Before presenting the results of our simulation work we summarize a few well-known predictions of the theory of activated processes. The main purpose is to draw the reader's attention to the best understood limits of system (1.1).

A. The multiplicative case (Refs. [15–18])

The Fokker-Planck equation corresponding to the Langevin equation (1.1) with δ correlated Gaussian noise sources $\xi(t)$ and $\eta(t)$ reads [18]

$$\frac{\partial}{\partial t}P(x,t)=\frac{\partial}{\partial x}[-ax+bx^3]P(x,t)+D\frac{\partial^2}{\partial x^2}P(x,t)+Q\frac{\partial}{\partial x}x\frac{\partial}{\partial x}xP(x,t), \tag{2.1}$$

where $P(x,t)$ is the probability distribution function of the stochastic process $x(t)$. For $D=0$ (purely multiplicative case) Eq. (2.1) can be solved analytically [16]. Its stationary solution $P(x)=P(x,t\to\infty)$ undergoes an abrupt transition from a bimodal to a monomodal distribution by increasing the noise intensity Q past the critical value $Q=a$ (noise induced transition). Examples of the distribution $P(x)$ for different values of the circuital parameters are reported in Sec. IV. In the absence of additive noise $D=0$, the Brownian particle is confined in one semiaxis ($x\geqslant 0$ or $x\leqslant 0$ according to the initial condition). A weak additive noise allows the particle to diffuse over the barrier at $x=0$. The relevant escape time, then, depends on both D and Q. However, since our simulations were performed at D constant, we agree to denote such an escape time by $T_0(Q)$. The dependence of T_0 on Q is well illustrated in Fig. 2 of Ref. [15]: $T_0^{-1}(0)$ coincides with the Kramers rate μ_K introduced for the purely additive case (see Sect. II B); $T_0^{-1}(Q)$ increases almost linearly with Q for $0\leqslant Q<a$ and, finally, diverges faster than exponentially for $Q>a$. An analytical treatment of $T_0(Q)$ has been reported recently in Ref. [10].

B. The additive case (Refs. [1, 18, 19])

A quantity which plays a crucial role in the present article is the escape (or Kramers) rate in a double-well potential driven by a purely additive noise $\xi(t)$. The archetypal Fokker-Planck equation (2.1) with $Q=0$ has been studied in great detail [1]. An approximate expression for the Kramers rate at low additive noise $D/E_0\ll 1$ reads [18]

$$\mu_K=\mu_0\exp(-E_0/D), \tag{2.2}$$

where the prefactor μ_0 is a weak function of the noise intensity. For the potential under investigation (1.1), $\mu_0=(a\sqrt{2}/\pi)(1-3D/8E_0+\cdots)$. In terms of the MFPT formalism, the reciprocal of μ_K coincides with the activation time T_K from one potential minimum $\pm x_m=\sqrt{a/b}$ up to the barrier top. On the other hand, μ_K closely approximates the first nonzero eigenvalue of the Fokker-Planck equation (2.1) with $Q=0$ [1]. For $aT_K\gg 1$ our experimental definition of the escape time (1.3) is consistent with the standard definition of the Kramers time $T_K=\mu_K^{-1}$ [18]. For the sake of a comparison, we recall that the MFPT between the two stable potential minima at $\pm x_m$, introduced for instance in Ref. [2], is just twice the Kramers time employed here.

C. The kinetic rate model

The kinetic rate model of activated processes allows us to address two opposite limits of fast and slow barrier fluctuations, respectively. Far from pretending to be exhaustive, we summarize here the basic results following the approach in Ref. [4]. Let us consider the simple case of a subthreshold dichotomic noise $\eta(t)$ (i.e., with $\sigma<a$). The effective potential $V(x)-x^2\eta(t)/2$ flips between two bistable configurations with barriers $E_\pm=(a\pm\sigma)^2/4b$. Here, it is assumed that the adjustment into either state takes place instantaneously after each switching event. This requires that the noise time constant is sufficiently large, that is $a\tau>1$. Correspondingly, two Kramers rates $\mu_\pm(\sigma)=T_\pm^{-1}(\sigma)$ over $E_\pm$ may be introduced according to Eq. (2.2). At time t, a Brownian particle has probability $n_\pm(t)$ to be in the state with barrier $E_\pm$ prior to activation (of course, equally distributed into the left and the right well). The transition between the two states $\pm$ occurs through two alternative paths: either the particle is thermally activated to the absorbing state at the barrier tops $E_\pm$, whence the Kramers escape mechanism with rates $\mu_\pm$, or the particle sits in one state as long as the dichotomic noise flips by changing sign with rate $1/2\tau$—see Eq. (1.2). Such a description leads to a linear system of two coupled ordinary differential equations for $n_\pm(t)$, that is,

$$\dot{n}_\pm=(1/2\tau)[-(1+2\tau\mu_\pm)n_\pm+n_\mp], \tag{2.3}$$

with initial conditions $n_\pm(0)=1/2$ in the stationary regime. The quantity $n_+(t)+n_-(t)$ denotes the probability that the Brownian particle, being with a 50-50 probability in either state $\pm$, has not yet reached the barrier top at time t. From the definition of the MFPT as $T=\int_0^\infty(n_++n_-)dt$, Bier and Astumian, after solving Eq. (2.3), eventually obtained

$$T=(\mu_++\mu_-+2/\tau)/2[\mu_+\mu_-+(\mu_++\mu_-)/2\tau]. \tag{2.4}$$

Two limits of Eq. (2.4) are remarkable: in the intermediate color regime $a\tau>1$ and $\tau\ll\mu_+^{-1}+\mu_-^{-1}$

$$T^{-1}(0,\sigma)=[\mu_+(\sigma)+\mu_-(\sigma)]/2 \tag{2.5}$$

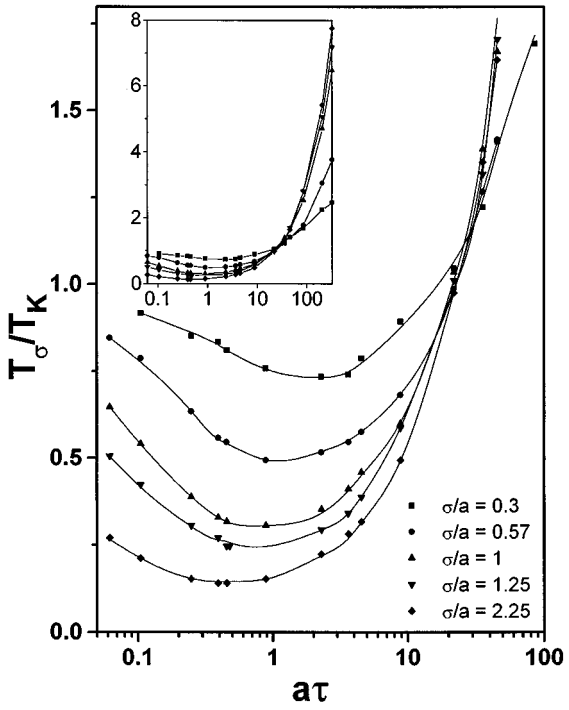

FIG. 1. G case: $T_\sigma(\tau)/T_K$ vs $a\tau$ for different values of σ/a. Other parameter values are $E_0/D=2.75$, $a=4.7\times10^3$ s^{-1}, and $T_K=8.5\times10^{-3}$ s.

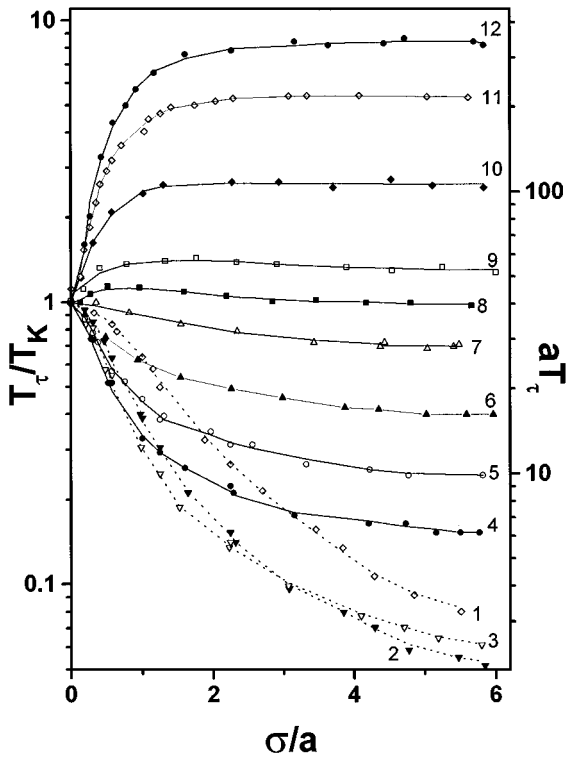

FIG. 2. G case: $T_\tau(\sigma)/T_K$ vs σ/a for $a\tau=0.05$ (curve 1), $=0.24$ (curve 2), $=0.48$ (curve 3), $=2.4$ (curve 4), $=4.8$ (curve 5), $=9.5$ (curve 6), $=19$ (curve 7), $=29$ (curve 8), $=43$ (curve 9), $=95$ (curve 10), $=240$ (curve 11), and $=360$ (curve 12). Other parameter values are as in Fig. 1.

and in the strong color regime $a\tau\to\infty$

$$T(\infty,\sigma)=[T_+(\sigma)+T_-(\sigma)]/2. \tag{2.6}$$

In the former limit the Kramers' notion of rate is tenable and the relevant MFPT coincides with the reciprocal of the average rate over the fluctuating barrier. In the latter limit, the effective potential $V(x)-x^2\eta(t)/2$ is almost static, so that a MFPT can be defined for any potential configuration. The rate notion is, then, lost and the stationary process MFPT is defined as the average MFPT over all individual barrier realizations. This important conclusion can be easily proved in the Fokker-Planck formalism, too, for any noise statistics [7,9].

The occurrence of RA is commonly associated with the crossover between the two limiting regimes (2.5) and (2.6). A simple estimate of the crossover noise correlation time follows from the interpretation of the Kramers prefactor μ_0 in Eq. (2.2) as an attack frequency, namely, as the number of unsuccessful escape attempts per unit of time the fluctuating particle makes in the average prior to a successful attempt. For $\mu_0\tau<1$ the Brownian particle during its escape attempts sees a rapidly fluctuating barrier, whereas for $\mu_0\tau>1$ it thermally fluctuates in an almost static potential.

III. RESONANT ACTIVATION

In Sec. II C we pointed out that for finite correlation times τ of the barrier fluctuation source (1.2), the escape time T depends on τ and σ, separately. Our simulation work was aimed at determining such a dependence over the broadest range of τ and σ values we could simulate. Our results are summarized in Figs. 1–7, where the curves $T_\sigma(\tau)$, $T_\tau(\sigma)$, and $T_Q(\tau)$ are displayed both for the G case (Figs. 1–3, 7) and the D case (Figs. 4–7). Here, the subscript of the three T functions denotes the quantity we kept constant, while varying the parameter that appears explicitly in their argument. Moreover, in our notation G case and D case stay for the system (1.1) with Gaussian and dichotomic noise source $\eta(t)$, respectively. For the reader's convenience, we remind him that the error magnitude on our measurements of T, $a\tau$, and σ/a was estimated to be smaller than 5% [12,13]. The

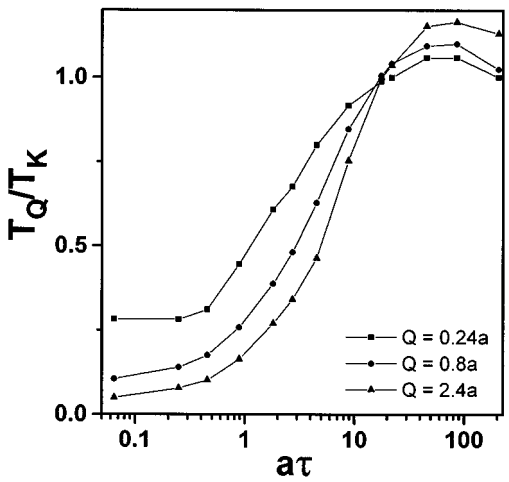

FIG. 3. G case: $T_Q(\tau)/T_K$ vs $a\tau$ for different values of Q. Other parameter values are as in Fig. 1.

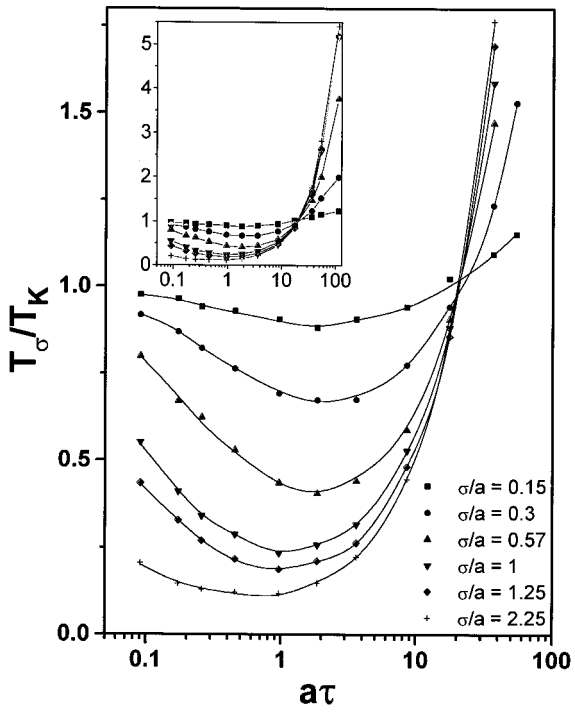

FIG. 4. *D* case: $T_\sigma(\tau)/T_K$ vs $a\tau$ for different values of σ/a. Other parameter values are as in Fig. 1.

main features of RA may be summarized as follows [12].

(i) Figure 1 for the *G* case and Fig. 4 for the *D* case display the RA phenomenon predicted by Doering and Gadoua [2]: The escape time $T_\sigma(\tau)$ hits a minimum for a certain

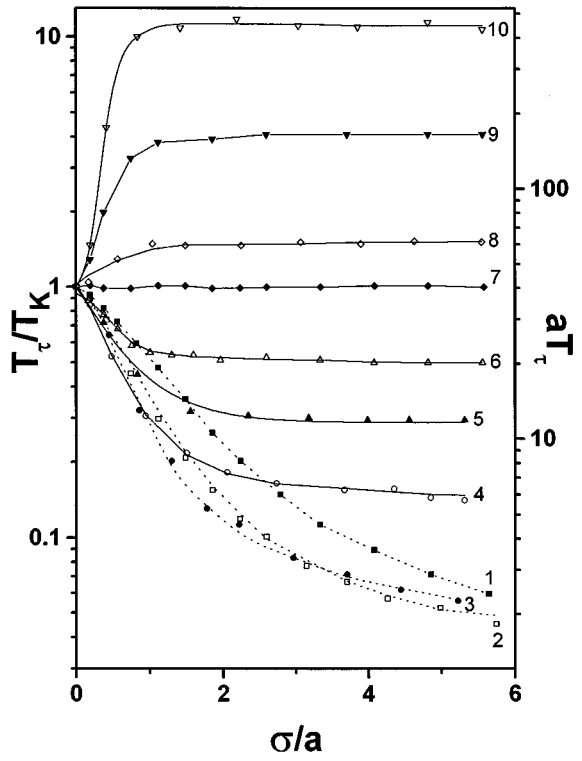

FIG. 5. *D* case: $T_\tau(\sigma)/T_K$ vs σ/a for $a\tau=0.1$ (curve 1), $=0.24$ (curve 2), $=0.48$ (curve 3), $=2.4$ (curve 4), $=4.8$ (curve 5), $=9.5$ (curve 6), $=19$ (curve 7), $=28$ (curve 8), $=86$ (curve 9), and $=240$ (curve 10). Other parameter values are as in Fig. 1.

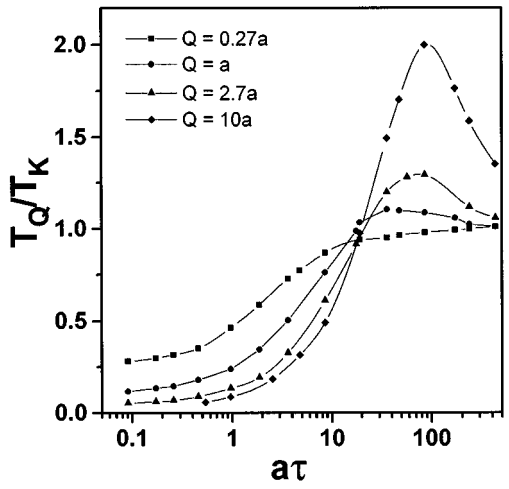

FIG. 6. *D* case: $T_Q(\tau)/T_K$ vs $a\tau$ for different values of Q. Other parameter values are as in Fig. 1.

value of the correlation time τ (denoted here by τ_{RA}), which proves to be a function of both σ and D. On increasing σ the RA minima shift towards smaller τ_{RA} values. Such an effect is more apparent in the *D* case. Note that in both cases $T_\sigma(\tau_{\mathrm{RA}})$ may be much larger than τ_{RA}, especially for subthreshold noises, contrary to predictions extrapolated from the simplified models of Refs. [3, 4]. Figure 7 shows that, on increasing the activation ratio E_0/D, the RA phenomenon is enhanced. The dip of the curve $T_\sigma(\tau)$ at τ_{RA} becomes deeper and shifts towards higher τ_{RA} values (almost inversely proportional to D). Such an enhancement, however, could not be clearly detected by plotting the ratio $T_\sigma(\tau)/T_K(D)$.

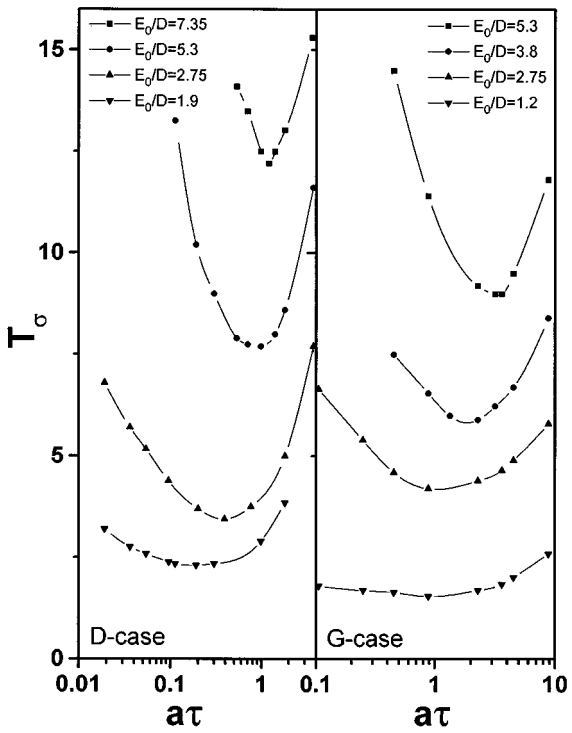

FIG. 7. $T_\sigma(\tau)$ vs $a\tau$ for $\sigma/a=0.57$ and different values of D. Other parameter values are as in Fig. 1.

(ii) In Figs. 1 and 4 several curves $T_\sigma(\tau)$ are drawn for different σ values. In the white noise limit $a\tau\to 0$, the multiplicative noise strength $Q=\sigma^2\tau$ tends to vanish so that all $T_\sigma(0)$ are expected to approach T_K, independently of the σ values. Our simulations seem to confirm this trend, even if we could not lower $a\tau$ below 0.05. In the opposite limit $a\tau\to\infty$, our data hint at infinitely large escape times with $T_\sigma(\tau)$ proportional to τ. Theoretical arguments [7,9] which apply to our model, too, would predict large but finite values for $T_\sigma(\infty)$. Unfortunately, we could not settle this point experimentally, due to the exceedingly large integration times required. Finally, all curves in Figs. 1 and 4 intersect one another for one value of the correlation time τ, $a\tau\simeq 20$, independently of the σ value and of the statistics of $\eta(t)$ (at least, within our experimental accuracy). At the intersection point T_σ equals T_K.

(iii) Figures 3 and 6 make it apparent that for a given barrier fluctuation strength Q, no RA occurs [12]. The curves $T_Q(\tau)$ all approach horizontal asymptotes for both $a\tau\to 0$ and $a\tau\to\infty$ [7,11]. In fact, for $a\tau\to 0$ we are in the white noise case studied in Ref. [15] and $T_Q(\tau)=T_0(Q)$ (see Sec. II A). In the strong color limit $a\tau\to\infty$, T_Q clearly converges to the finite value T_K. Note that for $Q\gtrsim a$ the curves $T_Q(\tau)$ develop a clear-cut maximum at large τ values. Moreover, they all intersect one another for the same value of the noise correlation time $a\tau=20$, where also curves $T_\sigma(\tau)$ do.

(iv) Figures 2 and 5 show the dependence of $T_\tau(\sigma)$ on σ. In the regime of weak $a\tau\ll 1$ to intermediate color $a^{-1}<\tau<T_K/2$, the curves $T_\tau(\sigma)$ fall off monotonically from the Kramers escape time $T_\tau(0)=T_K$, down to what looks like an asymptotic value $T_\tau(\infty)$. The modulus of the negative slope of $T_\tau(\sigma)$ at $\sigma=0+$, increases with τ, goes through a maximum and, then, decreases again. Consistently with the RA phenomenon item (i) for each value of σ there exists one value of the correlation time $\tau_{\rm RA}$ that sets a lower bound to the bundle of curves $T_\tau(\sigma)$. For values of τ of the order of $T_K/2$ and larger, the G and the D case exhibit differences which cannot be accommodated within the inaccuracies of the experimental setup. In both cases, the slope of $T_\tau(\sigma)$ is positive at $\sigma=0+$ and $T_\tau(\infty)$ defines an horizontal asymptote. However, while in the D case $T_\tau(\infty)$ approaches the limiting value 2τ over an $a\tau$ interval of at least two orders of magnitude, i.e., for $2<a\tau<2\times 10^2$, the behavior of $T_\tau(\infty)$ in the G case is more complicated. For extremely large τ values, say $\tau>2T_K$, the existence of the asymptote $T_\tau(\infty)\sim\tau$ is experimentally well assessed. For $\tau\sim T_K$ the approach of $T_\tau(\sigma)$ to an asymptotic value $T_\tau(\infty)$ is much slower, though our data suggest that for this range of the correlation times, too, $T_\tau(\sigma)$ ought to converge to values not much larger than τ. Finally, a remarkable similarity between the G and the D case in the weak noise limit: we verified that for $a\tau<1$, namely, for the interval $0.1<a\tau<0.5$ reported in Figs. 2 and 5, $T_\tau(\infty)$ becomes independent of τ and the multiplicative noise statistics. This result would imply that $T_0(Q)$ defined in Sec. II A tends to a finite limit for increasingly large Q values.

(v) In the range $\tau\sim T_K$ the curves $T_\tau(\sigma)$ in Fig. 2 reveal a further property of the G case, which is totally absent in the D case. These curves exhibit a maximum for a certain value of σ, which in turn increases with τ. Such an effect tends to disappear in the strong color limit. e.g., for $\tau>2T_K$.

Most of the above results have been tested also for different noise correlation function. For instance, on replacing the RC filter simulating the correlation function (1.2) for the G case by either a forth-order RC or an n-pole Butterworth filter with $n=2$, 4, and 8, we reproduced properties (i)–(iv), whereas the effect described in item (v) is wiped out [12].

IV. A QUALITATIVE INTERPRETATION

In this section we propose a simple interpretation of the results detailed in Sec. III, mostly based on qualitative or heuristic arguments. The approximate schemes of Refs. [7–11] would be, indeed, a viable tool to describe the RA phenomenon systematically. Unfortunately, the range of the τ and σ values explored in our simulation work is often too limited for a comparison with the theoretical predictions to be conclusive. For instance, the asymptotic predictions for $T_\sigma(\infty)$ and $T_\tau(\infty)$ in Ref. [7] and [9] are expected to become true for exceedingly large values of τ and σ, respectively. As a general rule, we present our interpretation of the simulation data following the same itemization as in Sec. III. Agreement (or disagreement) with the predictions of more refined analytical treatments will be mentioned explicitly.

(i) The occurrence of RA in system (1.1) is commonly justified as follows. In the weak color regime $a\tau\ll 1$, the small-τ expansion applies [18,19]: on increasing τ, the potential function $V(x)-x^2\eta(t)/2$ must be corrected into $\int^x V'(y)/(1+Qy^2/D)dy$, whence to first order in $a\tau$ [9]

$$T(\tau,\sigma)=T_K\exp\left[-(Q/D^2)\int_{-x_m}^{0}V'(x)x^2dx\right]$$
$$=T_K\exp[-(4a\tau/3)(\sigma/a)^2(E_0/D)^2]. \quad (4.1)$$

Equation (4.1) holds good for both the G and the D case provided that $a\tau\ll(D/E_0)(a/\sigma)^2$, corrections to the prefactor μ_0 have been neglected [10]. Hence, for small $a\tau$ the escape time decreases with increasing $a\tau$. In the opposite limit $\tau\gg T_K$, the strong color regime of Sec. II C predicts that the escape time $T(\tau,\sigma)$ be the average of the times required by the Brownian particle to diffuse over each barrier configuration [2]. Since T_K is proportional to the Arrhenius factor $\exp(E_0/D)$, the longest escape times dominate in the averaging procedure, whence $T(\tau,\sigma)>T_K$ for $\tau>T_K$. More precisely, to leading order in $1/a\tau$ and $(E_0/D)(\sigma/a)^2$

$$T_\sigma(\infty)=T_K\exp[2(\sigma/a)^2(E_0/D)^2] \quad (G \text{ case}) \quad (4.2)$$

and

$$T_\sigma(\infty)=T_K\cosh[2(\sigma/a)(E_0/D)] \quad (D \text{ case}). \quad (4.3)$$

Expressions for $T_\sigma(\infty)$ at larger σ values are proven below to verify the inequality $T_\sigma(\infty)>T_K$. The RA minimum of $T_\sigma(\tau)$ is thus expected to occur at the crossover between the two color limits, namely, for values of the noise correlation time τ of the order of the inverse attack frequency of the escaping Brownian particle out of a fluctuating well [9]—see Sec. II C. The rough estimate $a\tau_{\rm RA}\sim\pi/\sqrt{2}$ obtained from Eq. (2.2), fails to reproduce the D and σ dependence of $\tau_{\rm RA}$. As a matter of fact, Figs. 1 and 4 prove beyond any doubt that $1/a\tau_{\rm RA}$ increases almost linearly with σ/a over one order of magnitude, at least. Furthermore, Fig. 7 shows that $a\tau_{\rm RA}$ is

proportional to E_0/D in the small but significant interval (2.0–8.0). Anyway, the minimum of $T_\sigma(\tau)$ occurs in the broad interval $1<a\tau<aT_K/2$, where the intermediate color regime of Sec. II C applies and $T_\sigma(\tau)$ approximates the reciprocal of the escape rate averaged over all barrier realizations. For small noise strengths $(\sigma/a)^2<D/2E_0$

$$T_\sigma(a^{-1}\ll\tau\ll T_K)=T_K\exp[-2(E_0/D)^2(\sigma/a)^2] \quad (G \text{ case}) \tag{4.4}$$

and

$$T_\sigma(a^{-1}\ll\tau\ll T_K)=T_K/\cosh[(2E_0/D)(\sigma/a)] \quad (D \text{ case}). \tag{4.5}$$

Equations (4.4) and (4.5) provide a lower bound to $T_\sigma(\tau_{\mathrm{RA}})$. The present analysis seems to rule out RA as the signature of a well-defined resonance mechanism.

(ii) From Eq. (4.1) the white noise limit $a\tau\to0$ for $T_\sigma(\tau)$ in Figs. 1 and 4 reads $T_\sigma(0)=T_K$, as expected. Moreover, the condition for the validity of Eq. (4.1) $a\tau\ll(D/E_0)(a/\sigma)^2$ tells us why the approach of $T_\sigma(\tau)$ to T_K for $a\tau\to0$ is increasingly slower for large σ/a values. In the opposite limit $a\tau\to\infty$, the kinetic rate model predicts that $T_\sigma(\infty)$ is well approximated by Eqs. (4.2) and (4.3) for small noise intensities and by similar, more general expression for larger σ values. Our data, instead, show a linear dependence of $T_\sigma(\tau)$ on τ in the range of $30<a\tau<300$ (Figs. 1 and 4), which appear to be consistent with the asymptotic behavior of $T_\tau(\infty)$ at large τ (Figs. 2 and 5). However, the reader should be aware that the two limiting procedures do not commute, i.e., in principle, $T_\sigma(\infty)\neq T_\tau(\infty)$. The coincidence of the two limits, here, is possibly due to the fact that the $a\tau$ values obtainable in our simulator are not large enough for a conclusive statement about the asymptotic behavior of $T_\sigma(\tau)$ to be issued. In fact, digital simulations [9] suggest that $T_\sigma(\infty)$ is attained only for $a\tau>10^4$, that is well beyond the capabilities of our circuitry [13]. Finally, a peculiar feature of the family of curves plotted in Figs. 1 and 4 is the existence of the intersection point at about $a\tau=20$. On taking notice that $aT_K=40$ (both in the G and D case), this is equivalent to state that $T_\sigma(\tau)$ is independent of σ for $T_K=2\tau$. Correspondingly, in both Fig. 2 and 5 there should exists a horizontal curve $T_\tau(\sigma)=T_K$ for $\tau=T_K/2$. In the D case (Fig. 5) this effect is apparent, whereas in the G case (Fig. 2) a finer tuning of the control parameter τ would be needed to select an (almost) constant $T_\tau(\sigma)$—see item (iv) below.

(iii) The curves $T_Q(\tau)$ of Figs. 3 and 6 prove that no RA occurs for $Q=\sigma^2\tau$ constant, as predicted theoretically in Refs. [8] and [10]. Moreover, the two limiting values $T_Q(0)$ and $T_Q(\infty)$ are well explained in terms of the results of Sec. II. For $a\tau\to\infty$, the variance of the multiplicative noise $\sigma^2=Q/\tau$ vanishes, whence the barrier fluctuations do not affect the escape process any longer and $T_Q(\infty)=T_K$. For $a\tau\to0$, the white noise limit $T_0(Q)$ is recovered. Our data for $T_Q(0)$ are in qualitatively good agreement with predictions (2.7)–(2.9) of Ref. [10] and obey the same trend observed first in Ref. [15]. The occurrence of the $T_Q(\tau)$ maxima at large τ values can be easily explained on the ground of the arguments of items (i) and (ii); the asymptotic escape times (4.2) and (4.3) clearly indicate that $T_Q(\tau)$ is an increasing function of either Q/τ in the G case or $\sqrt{Q/\tau}$ in the D case. Moreover, all curves $T_Q(\tau)$ intersect one another at one point for the same reason why the curves $T_\sigma(\tau)$ do, so that their intersection point is located by $T_Q(T_K/2)=T_K$. Such a feature, not predicted by the approximate schemes [7–11], was recently reported in Ref. [20].

(iv) The behavior of $T_\tau(\sigma)$ at small σ/a values can be easily understood in terms of kinetic rate model of the escape process. In the weak color regime $a\tau\to0$ [more precisely, for $a\tau\ll1$ and $a\tau\ll(D/E_0)(a/\sigma)^2$] $T_\tau(0)$ is approximated by Eq. (4.1). Its negative slope increases in modulus with τ as observed experimentally. For very large τ values and $\sigma/a\to0$, instead, we observe that the curves $T_\tau(\sigma)$ in Figs. 2 and 5 become independent of the noise correlation time. According to the limiting regimes of the kinetic rate model

$$T_\tau(\sigma)=T_\sigma(a^{-1}\ll\tau\ll T_K) \tag{4.6}$$

for $1<a\tau<aT_K/2$ and

$$T_\tau(\sigma)=T_\sigma(\infty) \tag{4.7}$$

for $\tau>2T_K$ with $T_\sigma(a^{-1}\ll\tau\ll T_K)$ and $T_\sigma(\infty)$ for $(\sigma/a)^2\ll D/E_0$ given in Eqs. (4.4) and (4.5) and Eqs. (4.2) and (4.3), respectively. We note that for relatively large τ values ($a\tau>1$) $T_\tau(\sigma)$ approaches T_K either linearly (D case) or quadratically (G case) in σ/a. Such a difference becomes apparent by comparing Figs. 2 and 5.

The asymptotic behavior of $T_\tau(\sigma)$ for $\sigma/a\to\infty$ looks rather complicated. Standard calculations [10] based on the notion of rate make no sense at large σ/a values, since for $\sigma>a$ (D case) and $(\sigma/a)^2>D/2E_0$ (G case) the full bistability of the system is lost. Indeed, if we take the limit $\sigma/a\to\infty$ at large but finite τ values, the kinetic rate model should be applied with some caution. Our argument runs particularly simple in the D case. When $\eta(t)=+\sigma$, the effective barrier $E_+=(a+\sigma)^2/4b$ may be so high that the relevant escape time T_+ is by far too long, for the Brownian particle to escape from one well into the other within the time 2τ the dichotomic noise takes to flip from $+\sigma$ to $-\sigma$. When $\eta(t)=-\sigma$, no effective barrier exists for $\sigma>a$ and relaxation of the Brownian particle in the corresponding monostable well at $x=0$ occurs on a time scale of the order of $1/\sigma$ for $\sigma\gg a$ with $1/\sigma\ll\tau$ (barrier-no-barrier regime). It follows immediately that under these circumstances the escape time $T_\tau(\infty)$ is determined by the flipping time of the driving multiplicative noise, whence our prediction $T_\tau(\infty)=2\tau$ (D case) in both the intermediate and strong color regimes. In terms of the kinetic equations (2.3), this regime corresponds to setting $n_-\equiv0$ at any time, whence $T=2\tau/(1+2\mu_+\tau)$ with $\mu_+\tau\ll1$.

The generalization of the barrier-no-barrier picture to the G case is not straightforward. The noise correlation time is still expected to set the time constant of the process correlation function (related above to our escape time). It might be argued [21], though, that for $1<a\tau<aT_K/2$ the two-state mechanism outlined for the D case is a viable approximation to the G case, as well. The escape rate would be negligible for $\eta(t)>0$, due to the presence of the confining unperturbed barrier E_0, whereas relaxation would occur on a time scale much shorter than τ for $\eta(t)<0$. This remark would justify the approximate asymptote $T_\tau(\infty)=2\tau$ reported in Ref. [12] for the G case and the common intersection point of all the

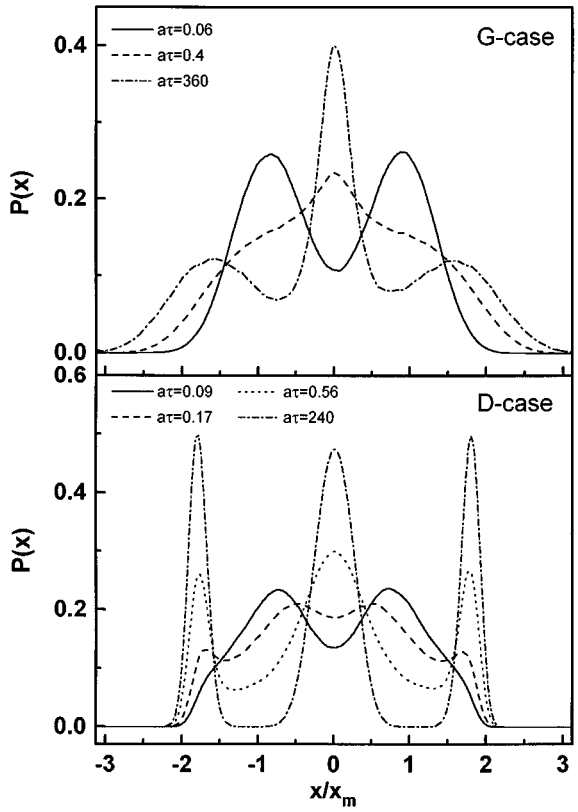

FIG. 8. $P(x)$ in the G and D case for different values of $a\tau$. Other parameter values are as in Fig. 1.

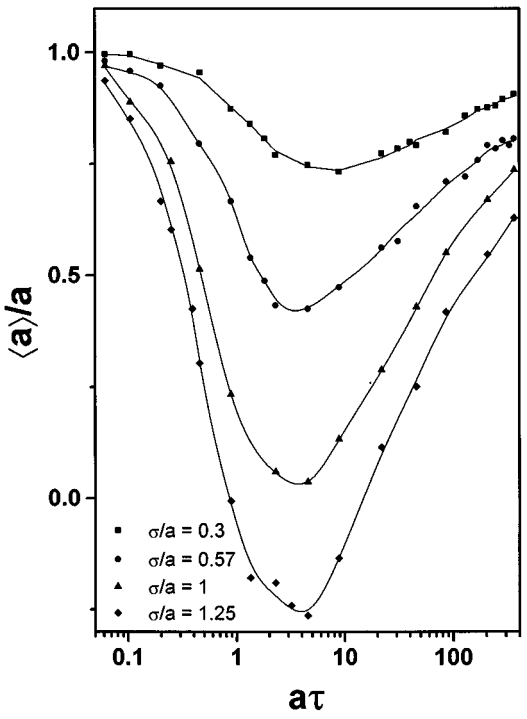

FIG. 9. G case: $\langle a\rangle=\overline{a_\sigma}(\tau)$ vs $a\tau$ for different values of σ/a. Other parameter values are as in Fig. 1.

$T_\tau(\sigma)$ curves at $\tau=T_K/2$—see item (iii). When τ grows much larger than T_K, the escape process takes place also for a substantial fraction of the barrier configurations with $\eta>0$. The two states $\pm$ cannot be identified uniquely (see Fig. 8); the Fokker-Planck equation for continuous processes becomes a more appropriate formalism. The global relaxation time would be, then, controlled directly by the correlation time of the driving noise, whence $T_\tau(\infty)=\tau$ (G case). The authors of Ref. [7] question the exponential nature of the $\langle x(t)x(0)\rangle$ decay itself. The accuracy of our simulation device does not allow to clarify this point any further.

Finally, we study the limit $T_\tau(\infty)$ in the weak color regime $a\tau\ll 1$. In such a regime $\eta(t)$ boils down to a white noise source with diverging strength, that is $Q\gg D$. As a consequence the action of the additive noise $\xi(t)$ is completely superseded by the effect of the multiplicative noise $\eta(t)$, so that the analysis in Ref. [17] for a purely multiplicative bistable system applies. It was proved there that the relaxation time (1.3) in a system like ours, (1.1), with no additive noise $D=0$, approaches a constant for $Q/a\to\infty$, namely,

$$aT_\tau(\infty)=\pi/2. \tag{4.8}$$

This prediction is closely verified for the first time by our simulations. Equation (4.8) applies both to the D and G case, since in the $a\tau\to 0$ limit with σ constant the effects of the noise statistics become indistinguishable [14]. Note that in this regime, too, the limits $a\tau\to 0$ and $\sigma/a\to\infty$ are not interchangeable—see item (ii).

(v) The bumps in the $T_\tau(\sigma)$ curves for $\tau\sim T_K$ are a peculiarity of the Ornstein-Uhlenbeck process $\eta(t)$ (1.2), and tend to disappear when n-pole filtering techniques are employed with $n\geqslant 2$. Such bumps are located at around $(\sigma/a)^2=D/2E_0$, thus marking the transition from strong color to the barrier-no-barrier regimes of the kinetic rate model. Analogously, in the D case $T_\tau(\sigma)$ reaches its asymptotic value 2τ for $\sigma\gtrsim a$, that is when full bistability is lost.

For reader's convenience, we display in Fig. 8 the probability distribution functions $P(x)$ of the stationary process $x(t)$ for a few significant choices of the parameters τ and σ. The difference between the D and the G case becomes apparent for large σ and τ values. In the D case the curves $P(x)$ for $a\tau\gg 1$ are clearly reproduced by the superposition of the probability distributions of two quasistationary processes with barrier configurations $E_\pm$, respectively. As a consequence, for $\sigma>a$ the curves $P(x)$ develop three sharp peaks corresponding to a probability 1/2 for the central peak and 1/4 for each side peak. In the G case curves $P(x)$ with three maxima are observable, too, but the relevant peaks, especially the side peaks, become very broad. Such a difference is related to the different asymptotic behavior of $T_\tau(\sigma)$ in Figs. 2 and 5 and of $\overline{a_\sigma}(\tau)$ in Figs. 9 and 10—see Sec. V.

V. THE TRAVERSAL BARRIER

To conclude we discuss now a new characterization of RA, which was suggested to us by a remark in Doering and Gadoua article [2]: ''In the neighborhood of the resonant activation, [...] the crossing occurs almost exclusively when the barrier is in the lower state.'' In order to give this statement a more quantitative footing we introduce here the notion of traversal barrier: any time the Brownian particle crosses the barrier level $x_b=0$ after having crossed it at time $t=0$, the relevant traversal time t_b and the instantaneous lin-

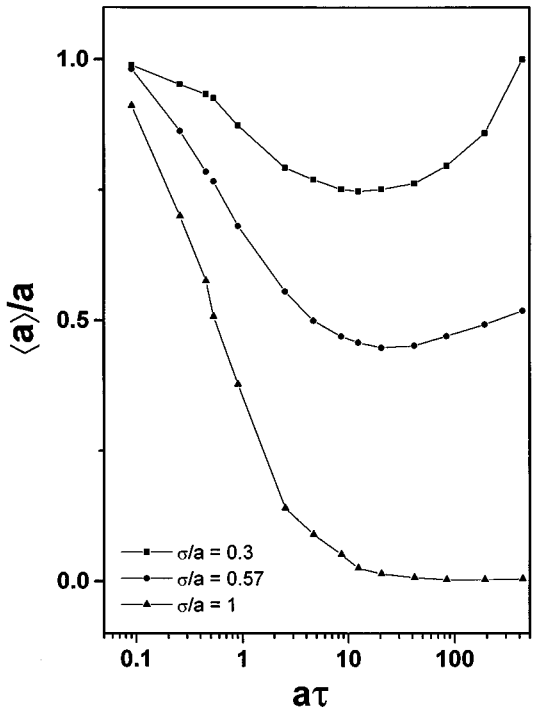

FIG. 10. D case: $\langle a\rangle=\overline{a_\sigma}(\tau)$ vs $a\tau$ for different values of σ/a. Other parameter values are as in Fig. 1.

ear drift coefficient $a+\eta(t_b)$ are recorded. Averages over as many as 10^4 level crossing events are taken to determine the distribution of t_b, and the traversal linear drift coefficient $\overline{a}=a+\overline{\eta}(t_b)$. Hence, for $\overline{a}$ positive definite, the corresponding traversal barrier reads $E=\overline{a}^2/4b$. Note that our definition of traversal barrier corresponds to a snapshot of $V(x)-x^2\eta(t)/2$ at time t_b, whereas the traversal process would require a finite time, possibly much larger than τ.

In Figs. 9 and 10 we plot $\overline{a}/a$ versus $a\tau$ for different values of σ/a in the D and G case, respectively. In both cases, on sweeping $a\tau$ through the entire range of simulated values, the function $\overline{a_\sigma}(\tau)$ goes through a minimum $\overline{a_m}$. The value of $\overline{a_m}$ is reasonably well approximated by the naive fitting law

$$\overline{a_m}/a=1-\sigma/a \tag{5.1}$$

for any value of σ/a. A significant difference between the two cases rises when we try to locate the minima of $\overline{a_\sigma}(\tau)$. In the G case, the relevant RA correlation time τ_{RA} seems to locate $\overline{a_m}$, as well (even when $\overline{a_m}$ is negative!), whereas in the D case the minima of $\overline{a_\sigma}(\tau)$ are much shallower, shifted towards much higher τ values and tend to disappear as σ approaches a.

The dependence of $\overline{a_\sigma}(\tau)$ on $a\tau$ can be represented as follows. In the weak color regime $a\tau\to 0$ and σ constant, the effect of the multiplicative noise becomes negligible, because its strength $Q=\sigma^2\tau$ tends to vanish. Hence, $\overline{a_\sigma}(\tau)$ approaches a independently of the value of σ. To study the finite correlation time regimes, we limit ourselves to the condition that full bistability is preserved, that is $(\sigma/a)^2<D/2E_0$ (G case) and $\sigma<a$ (D case). As for RA, we expect that the minimum of $\overline{a_\sigma}(\tau)$ occurs when the noise correlation time τ is of the order of the escape attempt time in the potential wells and, therefore, much shorter than the escape times over the $E_\pm$ barriers. As a consequence, the average traversal linear drift coefficient seen by the escaping particle in the intermediate color regime is

$$\overline{a_\sigma}=a-\langle\eta\mu(\eta)\rangle/\langle\mu(\eta)\rangle. \tag{5.2}$$

In the D case, the average $\langle\cdots\rangle$ is taken with respect to the two state distribution of the noise $\eta(t)$, that is, $(1/2)\delta(\eta-\sigma)$ and $\mu(\eta)$ is the escape rate over the barrier of the effective potential $V(x)-x^2\eta/2$. The average escape rates $\langle\mu(\eta)\rangle$ have been computed explicitly in Sec. IV for both noise statistics. Hence, our estimate for $\overline{a_m}$ in the D case reads

$$\overline{a_m}/a=1-(\sigma/a)\tanh[(2E_0/D)(\sigma/a)]. \tag{5.3}$$

Notice that our fitting law (5.1) follows Eq. (5.3) immediately for $D\ll E_0$ and σ/a constant (but, curiously enough, also for $\sigma\gg a$). In the G case, the average $\langle\cdots\rangle$ is taken with respect to a Gaussian distribution with variance σ^2. A straightforward calculation yields

$$\overline{a_m}/a=1/(1+z) \tag{5.4}$$

with $z=(2E_0/D)(\sigma/a)^2$ and $z\ll 1$. Predictions (5.3) and (5.4) turn out to reproduce closely our experimental data for $\overline{a_m}$, at least for not too large a σ/a value, as assumed in our averaging procedures.

In the strong color regime $\tau\gg T_K$, the escape process takes place over any barrier, no matter what its height. This implies that in the G case $\overline{a_\sigma}(\tau)$ increases substantially from its minimum value $\overline{a_m}$ up to close the unperturbed value a. This is not the case for a dichotomic noise $\eta(t)$ that switches between two values $\pm\sigma$, only.

One final remark: In the foregoing sections, we have considered the thermally activated process that occurs in a symmetric bistable potential coupled to an external noise source, the coupling being multiplicative (that is, even in potential notation). The symmetry of the ensuing stochastic process is thus preserved at any time. In fact, one might have considered the case of odd couplings, as well, where the external noise alters the symmetry of the effective potential randomly in time; for instance,

$$\dot{x}=-V'(x)+\xi(t)+\eta(t), \tag{5.5}$$

with $V(x)$, $\xi(t)$, and $\eta(t)$ defined by Eq. (1.1). It can be easily proven that even for such a process $T_\sigma(\tau)$ goes through a minimum. Thus, the phenomenon of RA occurs in a variety of circumstances where a thermally activated process is coupled to an external source of colored noise with correlation time of the order of the (unperturbed) system escape time.

[1] For a review, see P. Hänggi, P. Talkner, and M. Borkovec, Rev. Mod. Phys. **62**, 251 (1990); J. Maddox, Nature **359**, 771 (1992); T. Fonseca, J. A. N. F. Gomes, P. Grigolini, and F. Marchesoni, Adv. Chem. Phys. **62**, 389 (1985); J. Chem. Phys. **79**, 3320 (1983).

[2] C. R. Doering and J. C. Gadoua, Phys. Rev. Lett. **69**, 2318 (1992).

[3] U. Zürcher and C. R. Doering, Phys. Rev. E **47**, 3862 (1993).

[4] M. Bier and R. D. Astumian, Phys. Rev. Lett. **71**, 1649 (1993).

[5] C. Van den Broeck, Phys. Rev. E **47**, 4579 (1993).

[6] J. J. Brey and J. Casado-Pascual, Phys. Rev. E **50**, 116 (1994); W. Schneller, L. Gunther, and D. L. Weaver, *ibid.* **50**, 770 (1994).

[7] P. Pechukas and P. Hänggi, Phys. Rev. Lett. **73**, 2772 (1994).

[8] P. Hänggi, Chem. Phys. **180**, 157 (1994).

[9] P. Reimann, Phys. Rev. E **52**, 1579 (1995); Phys. Rev. Lett. **74**, 4576 (1995).

[10] A. J. R. Madureira, P. Hänggi, V. Buonomano, and W. A. Rodrigues, Jr., Phys. Rev. E **51**, 3849 (1995).

[11] R. Bartussek, A. J. R. Madureira, and P. Hänggi, Phys. Rev. E **52**, R2149 (1995).

[12] F. Marchesoni, L. Gammaitoni, E. Menichella-Saetta, and S. Santucci, Phys. Lett. A **201**, 275 (1995).

[13] F. Marchesoni, E. Menichella-Saetta, M. Pochini, and S. Santucci, Phys. Rev. A **37**, 3058 (1987).

[14] P. Hänggi, in *Noise in Nonlinear Dynamical Systems*, edited by F. Moss and P. E. V. McClintock (Cambridge University Press, Cambridge, England, 1989), p. 307.

[15] S. Faetti, P. Grigolini, and F. Marchesoni, Z. Phys. B **47**, 353 (1982).

[16] A. Schenzle and H. Brandt, Phys. Rev. A **20**, 1628 (1979).

[17] F. Marchesoni, Z. Phys. B **62**, 505 (1986); S. Faetti, C. Festa, L. Fronzoni, P. Grigolini, F. Marchesoni, and V. Palleschi, Phys. Lett. A **99**, 25 (1983).

[18] H. Risken, *The Fokker-Planck Equation* (Springer, Berlin, 1984).

[19] P. Hänggi, F. Marchesoni, and P. Grigolini, Z. Phys. B **56**, 333 (1984); P. Hänggi and P. Jung, Adv. Chem. Phys. **89**, 239 (1995), and references therein.

[20] J. Iwaniszewski (unpublished).

[21] It might be argued [12] that for intermediate color $1<a\tau\leqslant aT_K/2$, $T_\tau(\infty)$ seems to tend to 2τ as in the D case. This instance would result in a crossover from $T_\tau(\infty)=2\tau$ to $T_\tau(\infty)=\tau$ with increasing τ.